Supplementary Material

Composite Electrodes Based on Carbon Materials Decorated with Hg Nanoparticles for the Simultaneous Detection of Cd(II), Pb(II) and Cu(II)

Laia L. Fernández [1,2], Julio Bastos-Arrieta [3,4], Cristina Palet [1] and Mireia Baeza [2,*]

[1] GTS Research Group, Department of Chemistry, Faculty of Science, Edifici C-Nord, Universitat Autònoma de Barcelona, Carrer dels Til·lers, 08193 Bellaterra, Spain; laia.lopez@uab.cat (L.L.F); cristina.palet@uab.cat (C.P)
[2] GENOCOV Research Group, Department of Chemistry, Faculty of Science, Edifici C-Nord, Universitat Autònoma de Barcelona, Carrer dels Til·lers 08193, Bellaterra, Spain; mariadelmar.baeza@uab.cat (M.B.)
[3] Grup d'Electroanàlisi, Department of Chemical Engineering and Analytical Chemistry, Universitat de Barcelona, Carrer Martí i Franqués 1-11, 08028, Barcelona, Spain; julio.bastos@ub.edu (J.B.-A)

* Correspondence: mariadelmar.baeza@uab.cat (M.B.)

Table S1: Response of some modified electrodes and other analytical techniques.

Electrode	DL	Linear Range	Sensitivity	Ref
BiF/N/IL/G/SPCE	0.09 ng·mL^{-1} Zn^{2+} 0.06 ng·mL^{-1} Cd^{2+} 0.08 ng·mL^{-1} Pb^{2+}	0.1-100.0 ng·mL^{-1}	Cd^{2+}: 0.5189 μA·(ng·mL^{-1})$^{-1}$ Pb^{2+}: 0.3508 μA·(ng·mL^{-1})^{1} Zn^{2+}: 0.2137 μA·(ng·mL^{-1})$^{-1}$	[21]
Ultra trace graphite rotating disk with a film of Hg	0.8 ng·mL^{-1} Cd^{2+} 0.88 ng·mL^{-1} Pb^{2+}	Cd^{2+} and Pb^{2+}: 0-3 μg·L^{-1} Cu^{2+}: 0-10 μg·L^{-1}	Cd^{2+}: 5.46 μA·(μg·L^{-1})$^{-1}$ Pb^{2+}: 3.5 μA·(μg·L^{-1})$^{-1}$ Cu^{2+}: 1.21 μA·(μg·L^{-1})$^{-1}$	[22]
MCPE graphite/alginate	0.9 μg·L^{-1} Cd^{2+}	0.0-30.0 μg·L^{-1} Cd^{2+}	Cd^{2+}: 0.931 μA·(μg·L^{-1})$^{-1}$	[23]

Technique	DL	Ref
AAS	1 ng·mL^{-1} Cd 8 ng·mL^{-1} Pb 2 ng·mL^{-1} Cu	[10]
ICP-AES	0.007 ng·mL^{-1} Cd 1 ng·mL^{-1} Pb 0.04 ng·mL^{-1} Cu	
ICP-MS	<10 ng·mL^{-1} Cd <10 ng·mL^{-1} Pb <10 ng·mL^{-1} Cu	

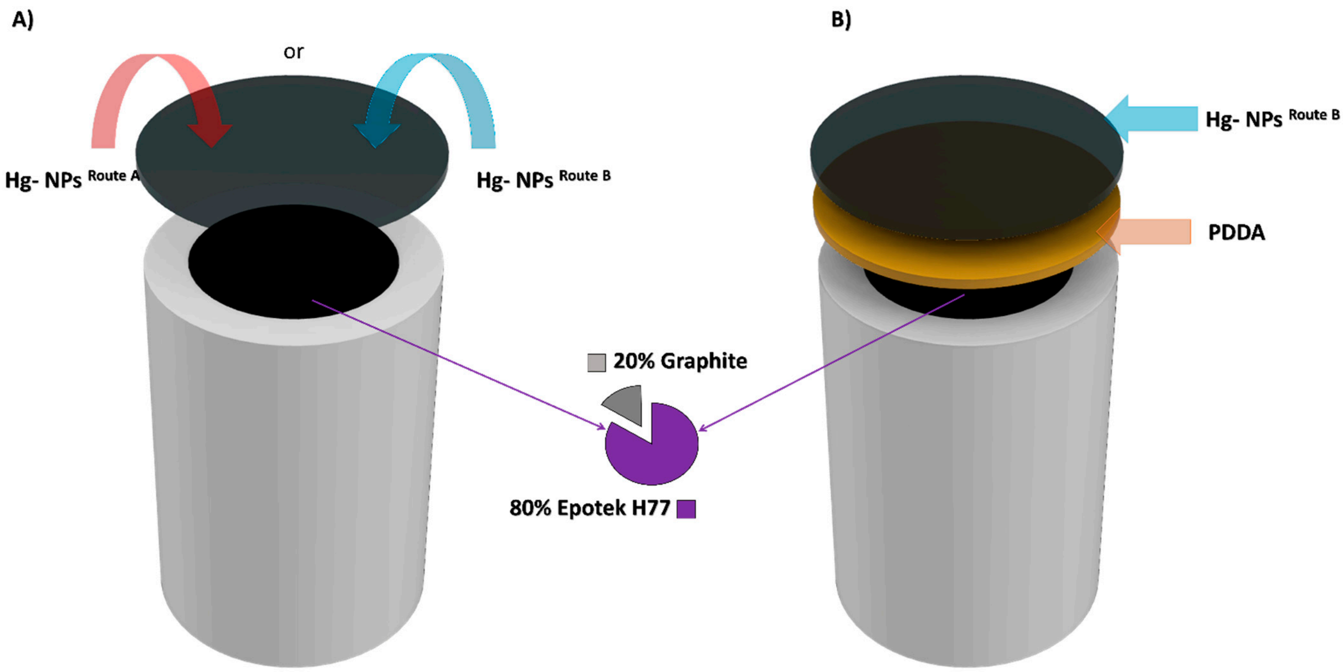

Figure S1: Scheme of the three types of electrodes.

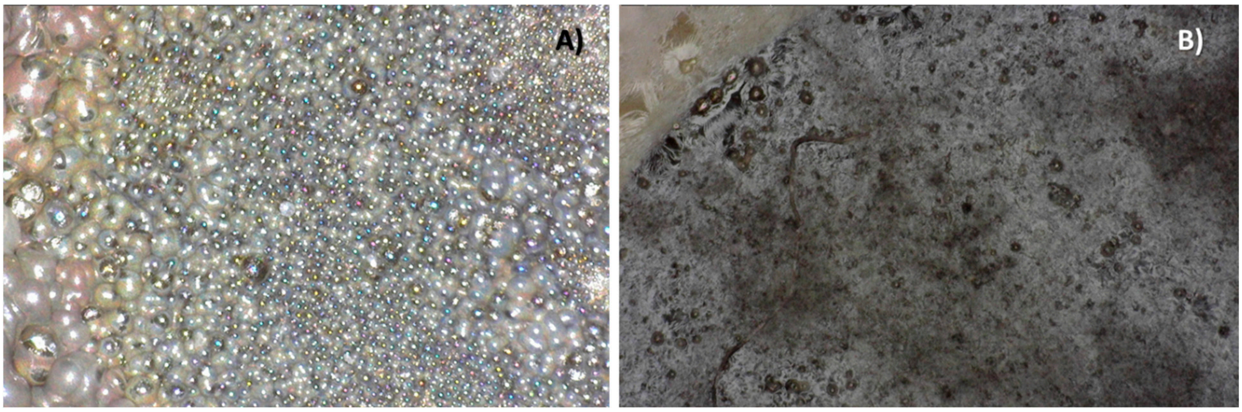

Figure S2. Using Dino-Lite Digital Microscope at 1:120 augments (A) Hg-NPs$^{Route\ B}$ @graphite electrode surface, and (B) Hg-NPs$^{Route\ A}$@graphite electrode surface.

Table S2: Data obtained from the adjustment of two components in the XPS analysis. Calibration made by using C at 284.8 eV.

Peak	Position	% at conc	Raw area
Hg 4f $_{7/2}$	101.32	58.33	7207.41
Hg 4f $_{5/2}$	105.35	41.67	5155.35

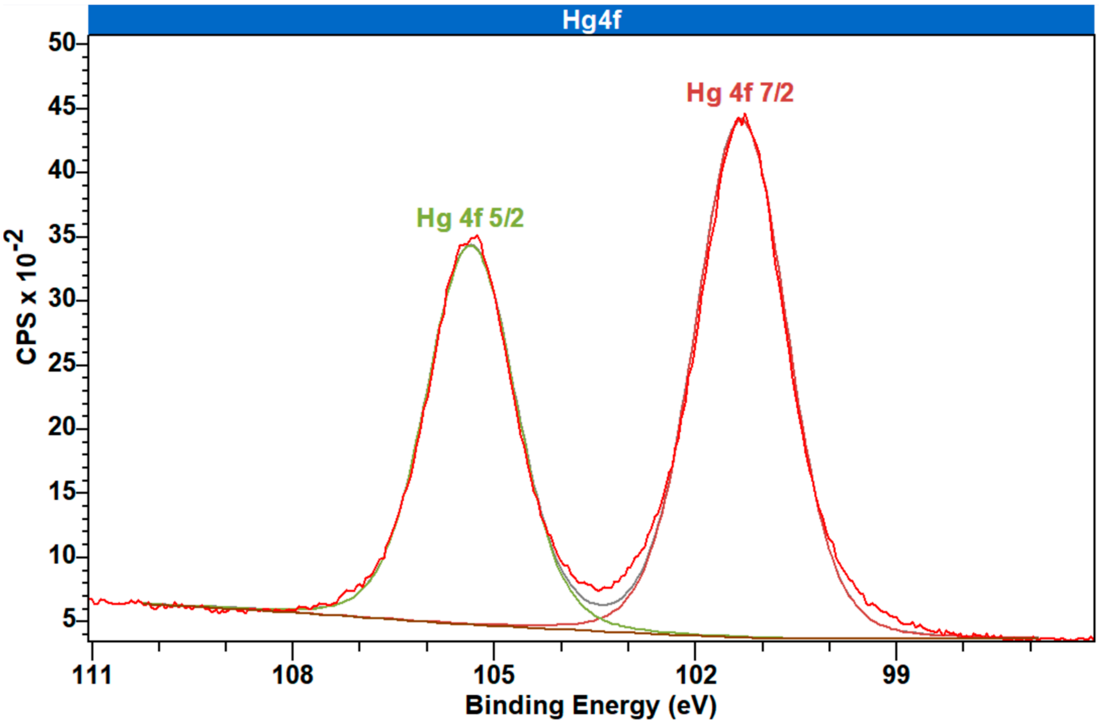

Figure S3: XPS analysis: adjustment for Hg 4f with two components: (green) for Hg 4f $_{5/2}$ and (red) for Hg4f $_{7/2}$.

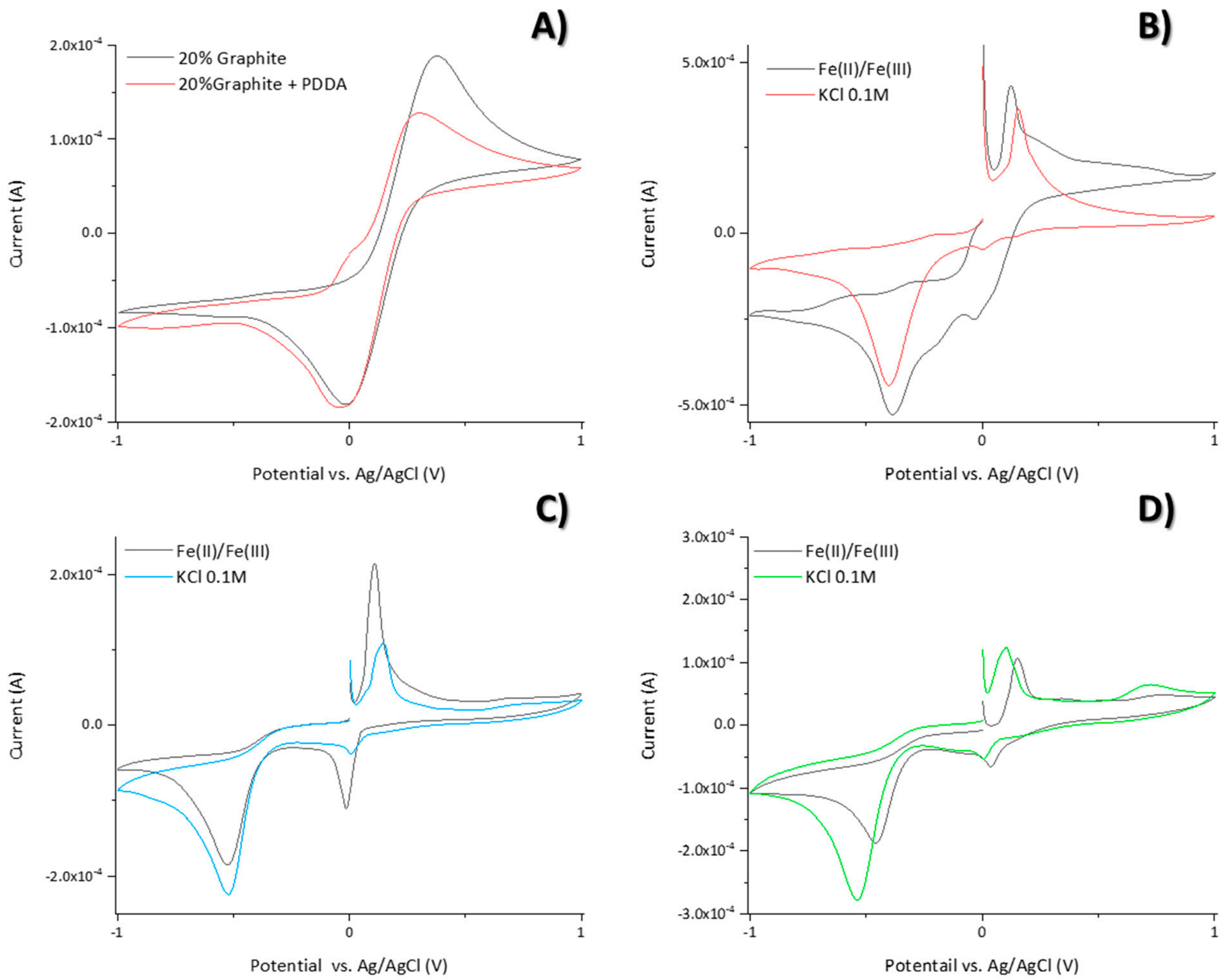

Figure S4: (A) CV using 0.01 M $[Fe(CN)_6]^{3-}/[Fe(CN)_6]^{4-}$, 0.1 M KCl with a 20% graphite electrode and 20% graphite electrode/PDDA. Comparison of the response in CV and in 0.01 M $[Fe(CN)_6]^{3-}/[Fe(CN)_6]^{4-}$, 0.1 M KCl and just 0.1 M KCl for (B) Hg-NPs$^{Route A}$ @graphite electrode; (C) Hg-NPs^{RouteB} @graphite electrode and (D) Hg- NPs^{RouteB}/PDDA @graphite electrode. Scan rate: 10 mV·s^{-1}.

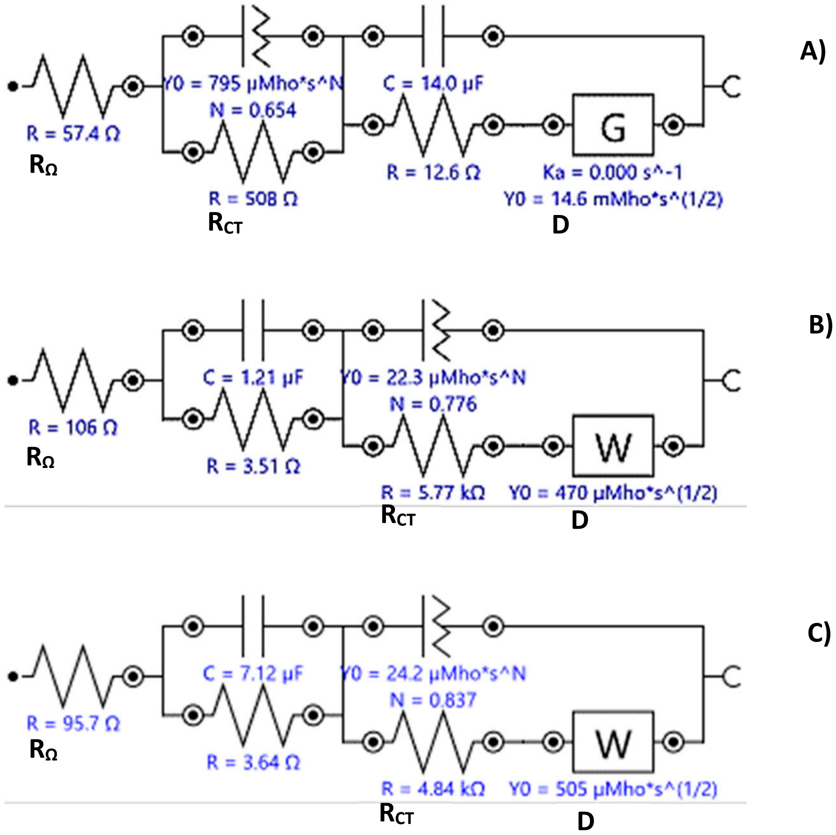

Figure S5: EIS adjusted circuits for: Hg-NPs$^{\text{Route A}}$ @graphite electrode (A); Hg-NPs$^{\text{Route B}}$ @graphite electrode (B); Hg-NPs$^{\text{Route B}}$/PDDA@graphite electrode (C). Where R_{Ω} is the ohmic resistance; R_{CT} is the charge transference resistance and D is the diffusion element chosen (G: Gerischer, W: Warburg).

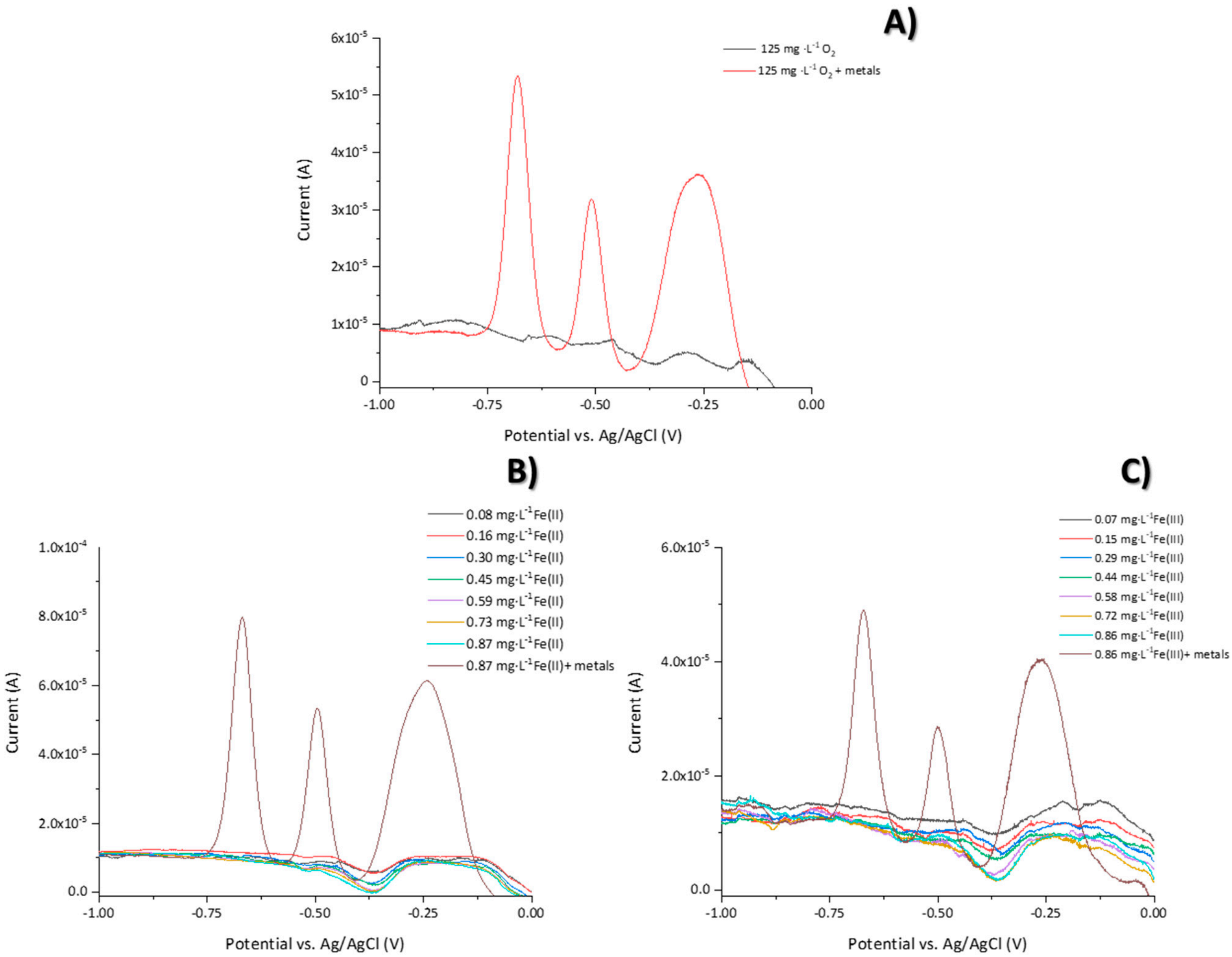

Figure S6: SWASV results of the addition for the interferences study: (A) dissolved organic matter; (B) Fe(II) and (C) Fe(III).